Eur. J. Mech., A/Solids, **17,** n° 3, 439-460, 1998

An anisotropic model of damage and frictional sliding for brittle materials

D. HALM * and A. DRAGON *

ABSTRACT. – The paper provides important developments for the model of anisotropic damage by mesocrack growth, accounting for unilateral behaviour relative to crack closure (Dragon and Halm, 1996, Halm and Dragon, 1996). Frictional sliding of closed microcrack systems is introduced here as an additional dissipative mechanism, which is considered to be coupled with the primary dissipative mechanism (damage by microcrack growth). Indeed, accounting for frictional sliding completes the description of moduli recovery in the existing model by adding to the normal moduli recovery effect (normal with respect to the crack plane) the substantial recovery of shear moduli. In parallel to damage modelling, the internal variable related to frictional sliding is a second-order tensor. Even if the unilateral effect and friction incipience are characterized by a discontinuity of effective moduli, it is crucial to ensure continuity of the energy and stress-response. Relevant conditions are proposed to ensure this. As far as frictional sliding is concerned, and unlike most of the models based on the classical Coulomb law, the corresponding criterion is given here in the space of thermodynamic forces representing a form of energy release with respect to the sliding internal variable. It appears that the normality rule in the latter space for sliding evolution is not physically contradictory with the observed phenomenon. The pertinence of the proposed theory, relative to the maximum dissipation hypothesis for both mechanisms, is illustrated by simulating loading paths involving damage and friction effects. © Elsevier, Paris

KEYWORDS. – Anisotropic damage, Frictional sliding, Moduli recovery, Coupling.

1. Introduction

The inelastic behaviour of a large class of solids commonly termed "brittle" (some rocks, concrete, ceramics, ...) is due to complex micro- and mesocrack growth coupled, eventually, with other dissipative phenomena, e.g. frictional sliding on crack faces. Multiple cracking under loading gives rise to secondary anisotropy, macroscopically observed irreversible strain, volumetric dilatancy as well as unilateral effects, *i.e.* recovery of elastic moduli corresponding to crack closure. The purpose here is to propose a new, non classical approach to model the joint process of frictional sliding and damage growth by microcracking. This is done under general loading conditions involving various dissipative configurations: frictional sliding at constant damage for closed microcracks, frictional sliding and evolving damage for closed microcracks, damage with no frictional sliding for open cracks, combinations of the above for multiple crack systems. The paper attempts to provide an efficient, reasonably simple, macroscopic model strongly motivated by physical considerations.

Existing theories frequently refer to micromechanical considerations with tractions on each mesocrack lip calculated from the applied stress, and the stress-strain relations derived by summation of contributions from individual cracks or crack sets. Friction is generally assumed to follow Coulomb law. A list of corresponding references would be too long to present here; in relation to this work it is appropriate to cite Andieux, 1981, Andrieux *et al.*, 1986, Fond and Berthaud, 1995, Gambarotta and Lagomarsino, 1993, Horii and Nemat-Nasser, 1983, Ju, 1991, Kachanov, 1982 and 1992, Krajcinovic *et al.*, 1994. Most of these analyses are limited to

* Laboratoire de Mécanique et de Physique des Matériaux (UMR CNRS 6617), ENSMA, Site du Futuroscope de Poitiers, BP 109, 86960 Futuroscope Cedex, France.

0997-7538/98/03/© Elsevier, Paris

two-dimensional, with the notable exception of the work by Gambarotta and Lagomarsino. Some references (e.g. Kachanov, 1982, Horii and Nemat-Nasser, 1983) give explicitly the influence of friction on the effective properties for specific loading paths.

The approach herein aims to complete the existing anisotropic damage model proposed by Dragon, see Dragon *et al.*, 1994, Dragon and Halm, 1996. The main features of this model are described in Section 2. In Section 3, frictional sliding is studied and a non-classical model is proposed, avoiding some inconveniences of Coulomb based formulations (Section 3.1-3.3). Then (Section 4), the crucial effect of damage/friction coupling is discussed. Some relevant simulations are presented to demonstrate the suitability of the model. The purpose of the modelling presented is to provide an efficient and consistent tool for nonlinear structural analysis which accounts for basic dissipative events in brittle solids. Emphasis is placed on reasonable simplicity and identifiability of material constants from accessible experimental data.

2. A model of anisotropic damage

This paragraph does not pretend to give the ins and outs of the anisotropic damage model which forms the starting point for further development (Section 3-4). Here, only the main features are summarized; for further details, *see* Dragon *et al.*, 1994, Dragon and Halm, 1996, and Halm and Dragon, 1996.

(i) In this section, the single dissipative mechanism considered is the generation and growth of decohesion mesosurfaces. This damage mechanism is described by a single second-order tensorial internal variable $\mathbf{D}$, displaying information about both the extent S (through scalar density $d^i(S)$) and orientation (normal $\mathbf{n}^i$) of the sets i of parallel crack-like defects:

$$\mathbf{D} = \sum_i d^i(S)\, \mathbf{n}^i \otimes \mathbf{n}^i \tag{1}$$

This form for the damage variable is motivated by micromechanics (*see*, for example, Kachanov, 1992). However, the term $d(S)$ has to be considered here as a macroscopic parameter and not as a microscopic quantity. Since $\mathbf{D}$ is a symmetric second-order tensor, it has three positive eigenvalues $D_k (k = 1, 2, 3)$ and three orthogonal eigenvectors $\boldsymbol{\nu}^k (k = 1, 2, 3)$, *i.e.* any influence of the damage configuration on the effective properties is considered to be coextensive to the influence of three equivalent mutually orthogonal families of parallel mesocracks characterized by D_k and the normal $\boldsymbol{\nu}^k$:

$$\mathbf{D} = \sum_{k=1}^{3} D_k\, \boldsymbol{\nu}^k \otimes \boldsymbol{\nu}^k \tag{2}$$

(ii) The thermodynamic potential (strain energy) contains linear terms in $\mathbf{D}$ (non-interacting crack hypothesis) and at most quadratic terms in $\boldsymbol{\varepsilon}$. A linear term in $\boldsymbol{\varepsilon}$ allows damage-induced residual phenomena to be taken into account (residual stress for $\boldsymbol{\varepsilon} = \mathbf{0}$ or residual strain for $\boldsymbol{\sigma} = \mathbf{0}$):

$$w = \frac{1}{2}\lambda (\operatorname{tr}\boldsymbol{\varepsilon})^2 + \mu \operatorname{tr}(\boldsymbol{\varepsilon}.\boldsymbol{\varepsilon}) + g \operatorname{tr}(\boldsymbol{\varepsilon}.\mathbf{D}) + \alpha \operatorname{tr}\boldsymbol{\varepsilon} \operatorname{tr}(\boldsymbol{\varepsilon}.\mathbf{D}) + 2\beta \operatorname{tr}(\boldsymbol{\varepsilon}.\boldsymbol{\varepsilon}.\mathbf{D}) \tag{3}$$

The equation of state defining the elastic behaviour given below introduces a form of damage-induced orthotropy through the terms preceded by the constants α and β:

$$\boldsymbol{\sigma} = \frac{\partial w}{\partial \boldsymbol{\varepsilon}} = \lambda (\operatorname{tr}\boldsymbol{\varepsilon})\mathbf{I} + 2\mu\boldsymbol{\varepsilon} + g\mathbf{D} + \alpha[\operatorname{tr}(\boldsymbol{\varepsilon}.\mathbf{D})\mathbf{I} + (\operatorname{tr}\boldsymbol{\varepsilon})\mathbf{D}] + 2\beta(\boldsymbol{\varepsilon}.\mathbf{D} + \mathbf{D}.\boldsymbol{\varepsilon}) \tag{4}$$

The expression for the thermodynamic force related to $\mathbf{D}$ is further decomposed into the two strain energy release terms related respectively to residual "locked" effects ($\mathbf{F}^{D1}$) and to recoverable energy ($\mathbf{F}^{D2}$). The former is decomposed into a splitting part $\mathbf{F}^{D1+}$ and a non-splitting part ($\mathbf{F}^{D1-}$):

$$
\begin{aligned}
(5) \qquad & \mathbf{F}^D = -\frac{\partial w}{\partial \mathbf{D}} = -g\boldsymbol{\varepsilon} - \alpha(\operatorname{tr}\boldsymbol{\varepsilon})\,\boldsymbol{\varepsilon} - 2\beta(\boldsymbol{\varepsilon}.\boldsymbol{\varepsilon}) \\
& \mathbf{F}^D = \mathbf{F}^{D1} + \mathbf{F}^{D2}; \quad \mathbf{F}^{D1} = -g\boldsymbol{\varepsilon}; \quad \mathbf{F}^{D2} = -\alpha(\operatorname{tr}\boldsymbol{\varepsilon})\,\boldsymbol{\varepsilon} - 2\beta(\boldsymbol{\varepsilon}.\boldsymbol{\varepsilon}) \\
& \mathbf{F}^{D1} = \mathbf{F}^{D1+} + \mathbf{F}^{D1-} = -g\boldsymbol{\varepsilon}^+ - g(\boldsymbol{\varepsilon} - \boldsymbol{\varepsilon}^+); \quad \boldsymbol{\varepsilon}^+ = \mathbf{P}^+ : \boldsymbol{\varepsilon}
\end{aligned}
$$

λ, μ, g, α, β are material parameters; $\mathbf{P}^+$ is a positive fourth-order projection tensor.

(iii) The equation of the elastic domain $f \leq 0$, written in $\mathbf{F}^D$-space, is assumed to be governed by the $\mathbf{F}^{D1+}$-part of $\mathbf{F}^D$, *i.e.* the splitting part of the "locked" damage energy release rate $\mathbf{F}^{D1}$ (by certain analogy with the stress deviator in classical plasticity):

$$
\begin{aligned}
(6) \qquad f(\mathbf{F}^D, \mathbf{D}) &= f(\mathbf{F}^D - \mathbf{F}^{D2} - \mathbf{F}^{D1-}, \mathbf{D}) \\
&= \sqrt{\frac{1}{2}\operatorname{tr}[(\mathbf{F}^D - \mathbf{F}^{D2} - \mathbf{F}^{D1-}) \cdot (\mathbf{F}^D - \mathbf{F}^{D2} - \mathbf{F}^{D1-})]} \\
&\quad + B\operatorname{tr}[(\mathbf{F}^D - \mathbf{F}^{D2} - \mathbf{F}^{D1-}) \cdot \mathbf{D}] - (C_0 + C_1 \operatorname{tr}\mathbf{D}) \leq 0
\end{aligned}
$$

B, C_0 and C_1 are material parameters.

The normality rule governing the damage growth has a strong physical sense since it relates the damage orientation to that of the tensile strain $\boldsymbol{\varepsilon}^+$, according to the splitting-like crack kinetics, and to the direction of the actual damage pattern:

$$
\begin{aligned}
(7) \qquad \dot{\mathbf{D}} &= \Lambda_D \frac{\partial f(\mathbf{F}^D - \mathbf{F}^{D2} - \mathbf{F}^{D1-}, \mathbf{D})}{\partial \mathbf{F}^D} \\
&= \begin{cases} \mathbf{0} & \text{if} \quad f < 0 \text{ or } f = 0,\ \dot{f} < 0 \\ \Lambda_D \left[\dfrac{\boldsymbol{\varepsilon}^+}{\sqrt{2\operatorname{tr}(\boldsymbol{\varepsilon}^+.\boldsymbol{\varepsilon}^+)}} + B\mathbf{D} \right] & \text{if} \quad f = 0 \text{ and } \dot{f} = 0 \end{cases}, \quad \Lambda_D \geq 0
\end{aligned}
$$

Remark. – B intervenes in the evolution law for $\mathbf{D}$ as a damage-drag constant: it prevents the $\mathbf{D}$-principal-axes from rotating abruptly.

Halm and Dragon, 1996, have further developed the model above in order to take into account the unilateral effect: under compressive loading, favorably oriented mesocracks may close, leading to an elastic moduli recovery phenomenon. According to the expression of the crack displacement discontinuity vectors, Kachanov, 1993, proves that the crack-density measure chosen here as the damage definition (1) is sufficient and rigorous in two-dimensional configurations and constitutes a good approximation for 3D cases, except for the case of cracks constrained against opening; in the latter case (1) is no longer sufficient and an additional fourth-order tensorial parameter plays a non-negligible role. Following this result, the constitutive equations of the model are

then rewritten, accounting for a new fourth-order parameter, designated here as $\hat{\mathbf{D}}$ and chosen in a particular manner, namely built upon the eigenvalues and eigenvectors of $\mathbf{D}$:

$$\hat{\mathbf{D}} = \sum_{k=1}^{3} D_k \, \boldsymbol{\nu}^k \otimes \boldsymbol{\nu}^k \otimes \boldsymbol{\nu}^k \otimes \boldsymbol{\nu}^k \tag{8}$$

An equivalent crack-system of normal $\boldsymbol{\nu}^k$ is called open if the corresponding normal strain is positive ($\boldsymbol{\nu}^k.\boldsymbol{\varepsilon}.\boldsymbol{\nu}^k > 0$), closed if it is zero or negative ($\boldsymbol{\nu}^k.\boldsymbol{\varepsilon}.\boldsymbol{\nu}^k \leq 0$), *see* Dragon and Halm, 1996, for details of this rigorous closure condition in the current framework. Then:

$$\begin{aligned} w = {} & \frac{1}{2}\lambda\,(\operatorname{tr}\boldsymbol{\varepsilon})^2 + \mu \operatorname{tr}(\boldsymbol{\varepsilon}.\boldsymbol{\varepsilon}) + g \operatorname{tr}(\boldsymbol{\varepsilon}.\mathbf{D}) + \alpha \operatorname{tr}\boldsymbol{\varepsilon} \operatorname{tr}(\boldsymbol{\varepsilon}.\mathbf{D}) + 2\beta \operatorname{tr}(\boldsymbol{\varepsilon}.\boldsymbol{\varepsilon}.\mathbf{D}) \\ & - (\alpha + 2\beta)\,\boldsymbol{\varepsilon} : \left[\sum_{k=1}^{3} H(-\boldsymbol{\nu}^k.\boldsymbol{\varepsilon}.\boldsymbol{\nu}^k)\, D_k \, \boldsymbol{\nu}^k \otimes \boldsymbol{\nu}^k \otimes \boldsymbol{\nu}^k \otimes \boldsymbol{\nu}^k\right] : \boldsymbol{\varepsilon} \end{aligned} \tag{9}$$

$$\begin{aligned} \boldsymbol{\sigma} = \frac{\partial w}{\partial \boldsymbol{\varepsilon}} = {} & \lambda\,(\operatorname{tr}\boldsymbol{\varepsilon})\,\mathbf{I} + 2\mu\,\boldsymbol{\varepsilon} + g\,\mathbf{D} + \alpha\,[\operatorname{tr}(\boldsymbol{\varepsilon}.\mathbf{D})\,\mathbf{I} + (\operatorname{tr}\boldsymbol{\varepsilon})\,\mathbf{D}] \\ & + 2\beta\,(\boldsymbol{\varepsilon}.\mathbf{D} + \mathbf{D}.\boldsymbol{\varepsilon}) \\ & - 2\,(\alpha + 2\beta) \sum_{k=1}^{3} H(-\boldsymbol{\nu}^k.\boldsymbol{\varepsilon}.\boldsymbol{\nu}^k)\, D_k\, (\boldsymbol{\nu}^k.\boldsymbol{\varepsilon}.\boldsymbol{\nu}^k)\, \boldsymbol{\nu}^k \otimes \boldsymbol{\nu}^k \end{aligned} \tag{10}$$

$$\begin{aligned} \mathbf{F}^D = -\frac{\partial w}{\partial \mathbf{D}} = {} & -g\boldsymbol{\varepsilon} - \alpha\,(\operatorname{tr}\boldsymbol{\varepsilon})\,\boldsymbol{\varepsilon} - 2\beta\,(\boldsymbol{\varepsilon}.\boldsymbol{\varepsilon}) \\ & + (\alpha + 2\beta) \sum_{k=1}^{3} H(-\boldsymbol{\nu}^k.\boldsymbol{\varepsilon}.\boldsymbol{\nu}^k).(\boldsymbol{\nu}^k.\boldsymbol{\varepsilon}.\boldsymbol{\nu}^k)^2\, \boldsymbol{\nu}^k \otimes \boldsymbol{\nu}^k \end{aligned} \tag{11}$$

Remark 1. – The coefficient $\alpha + 2\beta$ in front of the additional $\hat{\mathbf{D}}$-term has been rigorously determined by postulating that the initial stiffness of the undamaged solid is recovered in the direction normal to the closed mesocracks. The recovery of stiffness does not violate the continuity of the energy $w(\boldsymbol{\varepsilon}, \mathbf{D})$ (thermodynamic potential). In particular, in spite of the presence of the Heaviside function (which is discontinuous by nature), w, $\boldsymbol{\sigma}$, and $\mathbf{F}^D$ remain continuous when passing from the open mesocrack configuration to the closed mesocrack configuration (and vice versa).

Remark 2. – Since $\hat{\mathbf{D}}$ is derived from $\mathbf{D}$, it does not require a particular evolution law.

Remark 3. – Since any loading path is numerically considered as a collection of $\mathbf{D}$-proportional paths, Equation (11) is given for a fixed configuration of principal directions of $\mathbf{D}$, *i.e.*, on a $\mathbf{D}$-proportional segment.

3. Introduction of friction

The model presented in Section 2 is able to simulate a number of events related to damage by mesocracking (*see* for example Halm and Dragon, 1996, for a comparison between experiment and simulation). Among these phenomena, the unilateral effect explains moduli recovery in the direction normal to the closed cracks, but the

model fails to describe shear moduli recovery at the current time (*i.e.* a recovery in the direction colinear to the plane of the cracks); this implicitly corresponds to the hypothesis of perfectly lubricated cracks, where the frictional dissipation tends to zero. Nevertheless, this assumption is too strong in most of cases because of the roughness of the faces which slide with high dissipative friction. This frictional sliding leads to a blockage effect on the mesocracks, or, at least, to a reduction of the tangent displacement along the faces of the mesocracks on the microscale and to a substantial restoration of the shear stiffness at the macroscale. These effects are in addition to the normal moduli recovery process discussed above. This blockage effect has been observed by, for example, Pecqueur, 1995, who conducted torsional loading tests on hollow chalk cylinders first submitted to hydrostatic compression.

Unloading loops in Figure 1 exhibit hysteretic effects characterizing frictional blockage and sliding on closed mesocrack faces: the latter are first blocked by friction (quasi-vertical curve) and then progressively start to slide (decreasing slope). This effect was also commented on and accounted for in a two-dimensional micromechanically-based model by Andrieux *et al.*, 1986.

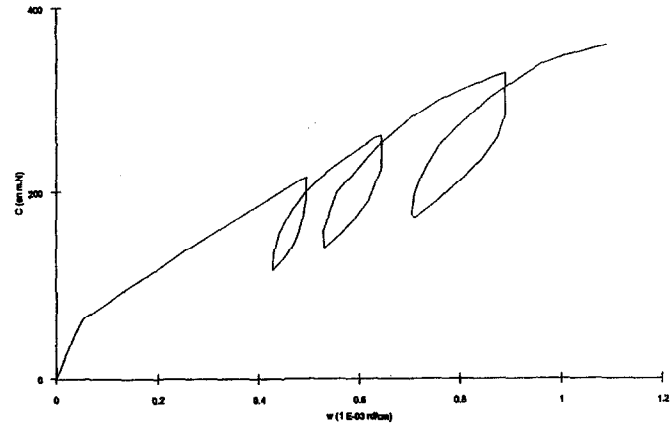

Fig. 1. – Torque C vs. angular strain w with loading/unloading (hydrostatic pressure of 8 MPa).

3.1. A NEW INTERNAL VARIABLE

Unlike Kachanov, 1982, or Horii and Nemat-Nasser, 1983, who just examine the influence of frictional sliding on the effective moduli, but, in fact, do not quantify the general sliding evolution (Kachanov gives a global expression for sliding in the stress subspace where it is not path-dependent), it appears imperative to describe completely the phenomenon, *i.e.* the amount and the direction of frictional sliding, in order to subsequently study the coupling of mesocracking and friction.

The expression of global strain for the Representative Volume Element (RVE) V giving explicitly the contribution ε^c of the cracks (assumed to be flat and quasi-circular) is:

$$\varepsilon = \mathbf{S}^0 : \sigma + \frac{1}{2V} \sum_i \left(\langle \mathbf{b} \rangle \otimes \mathbf{n} + \mathbf{n} \otimes \langle \mathbf{b} \rangle \right)^i S^i = \varepsilon^0 + \sum_i \varepsilon^{c\,i} \tag{12}$$

where $\mathbf{S}^0$ is the compliance tensor of the undamaged solid while the mesocrack i is characterized by its surface S^i, its normal $\mathbf{n}^i$ and its crack displacement discontinuity vector $\mathbf{b}^i$ ($\langle \mathbf{b}^i \rangle$ is $\mathbf{b}^i$ averaged over the whole crack i).

For closed sliding cracks, as long as damage axes do not evolve, $\langle \mathbf{b}^i \rangle$ reduces to a tangential component (*i.e.* $\langle \mathbf{b}^i \rangle$ is perpendicular to $\mathbf{n}^i$):

$$\langle \mathbf{b}^i \rangle = \xi^i \mathbf{g}^i \tag{13}$$

with $\mathbf{g}^i$ orthogonal to $\mathbf{n}^i$, if $\mathbf{n}^i$ remains constant. ξ^i is the amount of sliding in the direction $\mathbf{g}^i$. Then:

$$\boldsymbol{\varepsilon}^{c\,i} = \frac{S^i}{2V} \xi^i \left(\mathbf{g}^i \otimes \mathbf{n}^i + \mathbf{n}^i \otimes \mathbf{g}^i \right) \tag{14}$$

So, for the mesocrack i, the sliding internal variable is chosen as:

$$\boldsymbol{\gamma}^i = \frac{S^i \xi^i}{V} \operatorname{sym} (\mathbf{n} \otimes \mathbf{g})^i \tag{15}$$

sym ( ) means that the content of the parenthesis is symmetrized. Note the similarity with Equation (1): the form of $\boldsymbol{\gamma}$ is motivated by micromechanics but the quantity $\frac{S^i \xi^i}{V}$ cannot be explicitly calculated. According to the spectral decomposition (2), any set of mesocracks reduces to three equivalent systems; so, in a general case, $\boldsymbol{\gamma}$ includes three components corresponding to these three systems:

$$\boldsymbol{\gamma} = \sum_{k=1}^{3} \frac{S^k \xi^k}{V} sym (\nu \otimes \mathbf{g})^k = \sum_{k=1}^{3} \boldsymbol{\gamma}^k \tag{16}$$

where ν^k is the k-th **D**-eigenvector.

3.2. Elastic-damage response with friction

To simplify the problem, a single system of mesocracks is considered at the beginning of this section. The aim is to rewrite the thermodynamic potential to take into account recovery of the shear moduli due to blocking on the faces of closed mesocracks. The thermodynamic potential w has two different forms, the first is for open cracks (w^1 corresponding to Equation (9)), the other, w^2, is for closed cracks; the link between w^1 and w^2 being ensured by continuity considerations.

In Expressions (9)-(11), the β-term 2β tr $(\boldsymbol{\varepsilon}.\boldsymbol{\varepsilon}.\mathbf{D})$ in w is fully responsible for the degradation of the shear modulus. For example, consider a single mesocrack system, such that the normal to the cracks is in the x_3 direction; the shear stress is then:

$$\begin{cases} \sigma_{13} = 2\mu\, \varepsilon_{13} + 2\beta\, D_3\, \varepsilon_{13} \\ \sigma_{23} = 2\mu\, \varepsilon_{23} + 2\beta\, D_3\, \varepsilon_{23} \end{cases} \tag{17}$$

Note that the β-term (together with the α-term) contributes also to the reduction of the stiffness in the direction normal to the open crack set. This influence of α and β clearly appears in the expression of Young's modulus E_3 when considering the same damage configuration as above (one mesocrack system with normal in the x_3 direction):

$$E_3 = \lambda + 2\mu + 2\alpha D_3 + 4\beta D_3 - \frac{(\lambda + \alpha D_3)^2}{\lambda + \mu} \tag{18}$$

For further details on the expressions of the effective moduli, *see* Pham, 1994, or the Appendix.

If the mesocracks are blocked, the shear modulus 2μ is restored, corresponding to $\beta = 0$; so, the β-term will not appear in w^2. The α-term, which has no influence on shear moduli, remains unchanged. w^2 will furthermore be completed by invariant terms including the new internal variable γ. In these additional invariants, γ cannot appear without accompanying $\mathbf{D}$, since there is no sliding along the crack faces if there is no damage. Because of the definition (15), requiring that $\operatorname{tr}\gamma = 0$ and $\operatorname{tr}(\gamma.\mathbf{D}) = 0$ if damage axes do not evolve, only two simultaneous invariants of ε, γ and $\mathbf{D}$ provide pertinent information:

$$\operatorname{tr}(\varepsilon.\gamma.\mathbf{D}) \qquad \text{and} \qquad \operatorname{tr}(\gamma.\gamma.\mathbf{D}) \tag{19}$$

w^1 and w^2 have the following forms, considering first a single mesocrack set of normal ν:

$$w^1(\varepsilon, \mathbf{D}) = \frac{1}{2}\lambda(\operatorname{tr}\varepsilon)^2 + \mu\operatorname{tr}(\varepsilon.\varepsilon) + g\operatorname{tr}(\varepsilon.\mathbf{D}) + \alpha\operatorname{tr}\varepsilon\operatorname{tr}(\varepsilon.\mathbf{D}) + 2\beta\operatorname{tr}(\varepsilon.\varepsilon.\mathbf{D}) \tag{20a}$$

$$\begin{aligned} w^2(\varepsilon, \mathbf{D}, \gamma) = {} & \frac{1}{2}\lambda(\operatorname{tr}\varepsilon)^2 + \mu\operatorname{tr}(\varepsilon.\varepsilon) + g\operatorname{tr}(\varepsilon.\mathbf{D}) \\ & + \alpha\operatorname{tr}\varepsilon\operatorname{tr}(\varepsilon.\mathbf{D}) + 2\beta\operatorname{tr}(\varepsilon.\varepsilon.\mathbf{D}) - (\alpha + 2\beta)\,\varepsilon : \hat{\mathbf{D}} : \varepsilon \\ & + 2\beta\,\varepsilon : \hat{\mathbf{D}} : \varepsilon - 2\beta\operatorname{tr}(\varepsilon.\varepsilon.\mathbf{D}) \\ & + \eta_1\operatorname{tr}(\varepsilon.\gamma.\mathbf{D}) + 2\eta_2\operatorname{tr}(\gamma.\gamma.\mathbf{D}) \end{aligned} \tag{20b}$$

η_1 and η_2 are material parameters, to be identified a priori. The first two lines of Equation (20*b*) come from (9), *i.e.* the part of w which accounts for unilateral behaviour. The third and fourth lines represent the contribution from frictional sliding. It consists of two additional invariants containing γ, the term $2\beta\operatorname{tr}(\varepsilon.\varepsilon.\mathbf{D})$ preceded by the minus sign and cancelling the effects of the β-term in the second line and finally the term $2\beta\,\varepsilon : \hat{\mathbf{D}} : \varepsilon$, which cancels the corresponding negative term in the second line (indeed, the presence of this latter term is no longer necessary, since its role was to restore the normal stiffness reduced by the β-term in the second line).

Consider crack closure. Physically and microscopically, a multitude of crack closure modes has to be considered (Figure 2a): any closing path resulting from the open mesocrack configuration to the closed mesocrack configuration is conceivable (there is an infinity of such paths...). Nevertheless, the macroscopic continuity has to be ensured for the thermodynamic potential w and for the stress σ. To achieve this condition, we consider that a crack may close straight (Figure 2b) or slantwise (Figure 2c).

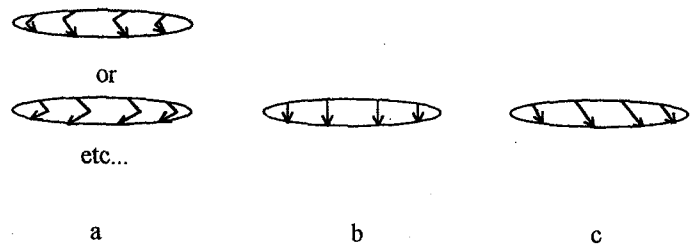

Fig. 2. – Crack closure modes.

In case b, there is no initial sliding ($\gamma = 0$), whereas in case c, the crack closes with a given initial quantity of sliding ($\gamma \neq 0$). This leads to the following condition: at closure, ε and γ have the same components in the crack plane; this can be written as:

$$\begin{cases} \varepsilon.\mathbf{D} = \gamma.\mathbf{D} \\ \mathbf{D}.\varepsilon = \mathbf{D}.\gamma \end{cases} \tag{21}$$

Equation (21) is synthesized in:

$$\gamma_{ij} = \mathrm{sym}\,(\varepsilon_{ik}\,\nu_k\,\nu_j) \quad \text{at the closure point} \tag{22}$$

Equation (22) acts as an initialization for the sliding variable.

As already emphasized in Halm and Dragon, 1996, the continuity of strain energy – and of corresponding stress response – has to be ensured in strain space on the strain "separation" surface of equation $\tilde{g}(\varepsilon) = \nu.\varepsilon.\nu = 0$ corresponding to crack opening/closure. The continuity conditions are given in Wesolowski, 1969, or Curnier *et al.*, 1995 for multilinear elasticity. In particular, the elasticity discontinuity operator $[[\mathbf{C}]] = \frac{\partial^2 w^1}{\partial\varepsilon\,\partial\varepsilon} - \frac{\partial^2 w^2}{\partial\varepsilon\,\partial\varepsilon}$ has to be singular: the dimension of its image is one. Accounting for the comments above and Relation (22), the jump $[[\mathbf{C}]]$ can be written as:

$$[[C]]_{ijkl} = \left(\frac{1}{2}\eta_1 + \eta_2 - \beta\right)(\delta_{ik}\,D_{jl} + \delta_{jl}\,D_{ik} + \delta_{il}\,D_{jk} + \delta_{jk}\,D_{il}) - 2\alpha\,\hat{D}_{ijkl} \tag{23}$$

A simple condition for $[[\mathbf{C}]]$ being of rank one ($\dim \mathrm{Im}\,[[\mathbf{C}]] = 1$) is:

$$\frac{1}{2}\eta_1 + \eta_2 - \beta = 0 \tag{24}$$

The potential w is therefore continuous on the surface $\tilde{g}(\varepsilon) = 0$ if the stress exhibits only a jump which is orthogonal to this surface. The condition here is stronger: no stress jump is allowed, which leads, after calculation and accounting for (22):

$$\eta_1 = 4\beta \tag{25}$$

To summarize the continuity conditions, w takes the following form:

$$\begin{aligned} w(\varepsilon, \mathbf{D}, \gamma) = {} & \frac{1}{2}\lambda\,(\mathrm{tr}\,\varepsilon)^2 + \mu\,\mathrm{tr}\,(\varepsilon.\varepsilon) + g\,\mathrm{tr}\,(\varepsilon.\mathbf{D}) \\ & + \alpha\,\mathrm{tr}\,\varepsilon\,\mathrm{tr}\,(\varepsilon.\mathbf{D}) + 2\beta\,\mathrm{tr}\,(\varepsilon.\varepsilon.\mathbf{D}) \\ & + H(-\nu.\varepsilon.\nu)[-\alpha\,\varepsilon : \hat{\mathbf{D}} : \varepsilon - 2\beta\,\mathrm{tr}\,(\varepsilon.\varepsilon.\mathbf{D}) \\ & \qquad + 4\beta\,\mathrm{tr}\,(\varepsilon.\gamma.\mathbf{D}) - 2\beta\,\mathrm{tr}\,(\gamma.\gamma.\mathbf{D})] \end{aligned} \tag{26}$$

η_2 being calculated above from (24), accounting for (25).

This relation is generalized to three non-interactive equivalent crack system of normal $\boldsymbol{\nu}^k$ (eigenvectors of $\mathbf{D}$, associated to the eigenvalues D_k, $k = 1,2,3$), by introducing a fourth-order tensor $\mathbf{L}^k$ which selects the k-th equivalent set:

$$\mathbf{L}^k = \boldsymbol{\nu}^k \otimes \boldsymbol{\nu}^k \otimes \boldsymbol{\nu}^k \otimes \boldsymbol{\nu}^k \tag{27}$$
$$\mathbf{D}^k = D_k \boldsymbol{\nu}^k \otimes \boldsymbol{\nu}^k = \mathbf{L}^k : \mathbf{D}$$

Then:

$$\begin{aligned} w(\boldsymbol{\varepsilon}, \mathbf{D}, \boldsymbol{\gamma}) = {} & \frac{1}{2}\lambda (\operatorname{tr}\boldsymbol{\varepsilon})^2 + \mu \operatorname{tr}(\boldsymbol{\varepsilon}.\boldsymbol{\varepsilon}) + g \operatorname{tr}(\boldsymbol{\varepsilon}.\mathbf{D}) + \alpha \operatorname{tr}\boldsymbol{\varepsilon} \operatorname{tr}(\boldsymbol{\varepsilon}.\mathbf{D}) \\ & + 2\beta \operatorname{tr}(\boldsymbol{\varepsilon}.\boldsymbol{\varepsilon}.\mathbf{D}) + \sum_{k=1}^{3} H(-\boldsymbol{\nu}^k.\boldsymbol{\varepsilon}.\boldsymbol{\nu}^k) \\ & \times [-\alpha\, \boldsymbol{\varepsilon} : (D_k \mathbf{L}^k) : \boldsymbol{\varepsilon} - 2\beta \operatorname{tr}(\boldsymbol{\varepsilon}.\boldsymbol{\varepsilon}.\mathbf{D}^k) + 4\beta \operatorname{tr}(\boldsymbol{\varepsilon}.\boldsymbol{\gamma}^k.\mathbf{D}^k) \\ & - 2\beta \operatorname{tr}(\boldsymbol{\gamma}^k.\boldsymbol{\gamma}^k.\mathbf{D}^k)] \end{aligned} \tag{28}$$

Note that this formulation allows each set to be dealt with independently, with all cases being possible (open or closed, sliding or non sliding sets).

The stress is determined by differentiating Equation (28):

$$\begin{aligned} \boldsymbol{\sigma} = \frac{\partial w}{\partial \boldsymbol{\varepsilon}} = {} & \lambda (\operatorname{tr}\boldsymbol{\varepsilon})\mathbf{I} + 2\mu\boldsymbol{\varepsilon} + g\mathbf{D} + \alpha[\operatorname{tr}(\boldsymbol{\varepsilon}.\mathbf{D})\mathbf{I} + (\operatorname{tr}\boldsymbol{\varepsilon})\mathbf{D}] \\ & + 2\beta(\boldsymbol{\varepsilon}.\mathbf{D} + \mathbf{D}.\boldsymbol{\varepsilon}) + \sum_{k=1}^{3} H(-\boldsymbol{\nu}^k.\boldsymbol{\varepsilon}.\boldsymbol{\nu}^k) \\ & \times [-2\alpha D_k (\boldsymbol{\nu}^k.\boldsymbol{\varepsilon}.\boldsymbol{\nu}^k)\boldsymbol{\nu}^k \otimes \boldsymbol{\nu}^k - 2\beta(\boldsymbol{\varepsilon}.\mathbf{D}^k + \mathbf{D}^k.\boldsymbol{\varepsilon}) \\ & + 2\beta(\boldsymbol{\gamma}^k.\mathbf{D}^k + \mathbf{D}^k.\boldsymbol{\gamma}^k)] \end{aligned} \tag{29}$$

The thermodynamic force related to $\mathbf{D}$ is (this expression is valid for $\mathbf{D}$-proportional paths, *see* Remark 3 following Equation 11):

$$\begin{aligned} \mathbf{F}^D = -\frac{\partial w}{\partial \mathbf{D}} = {} & -g\boldsymbol{\varepsilon} - \alpha(\operatorname{tr}\boldsymbol{\varepsilon})\boldsymbol{\varepsilon} - 2\beta(\boldsymbol{\varepsilon}.\boldsymbol{\varepsilon}) + \sum_{k=1}^{3} H(-\boldsymbol{\nu}^k.\boldsymbol{\varepsilon}.\boldsymbol{\nu}^k) \\ & \times [\alpha(\boldsymbol{\nu}^k.\boldsymbol{\varepsilon}.\boldsymbol{\nu}^k)^2 \boldsymbol{\nu}^k \otimes \boldsymbol{\nu}^k + 2\beta \mathbf{L}^k : (\boldsymbol{\varepsilon}.\boldsymbol{\varepsilon}) - 4\beta \mathbf{L}^k : (\boldsymbol{\varepsilon}.\boldsymbol{\gamma}^k) \\ & + 2\beta \mathbf{L}^k : (\boldsymbol{\gamma}^k.\boldsymbol{\gamma}^k)] \end{aligned} \tag{30}$$

Since the equivalent system of normal $\boldsymbol{\nu}^k$ has to be considered independently, a proper thermodynamic force $\mathbf{F}^{\gamma k}$ is associated with each variable $\boldsymbol{\gamma}^k$:

$$\mathbf{F}^{\gamma k} = -\frac{\partial w}{\partial \boldsymbol{\gamma}^k} = H(-\boldsymbol{\nu}^k.\boldsymbol{\varepsilon}.\boldsymbol{\nu}^k)[-2\beta(\boldsymbol{\varepsilon}.\mathbf{D}^k + \mathbf{D}^k.\boldsymbol{\varepsilon}) + 2\beta(\boldsymbol{\gamma}^k.\mathbf{D}^k + \mathbf{D}^k.\boldsymbol{\gamma}^k)] \tag{31}$$

3.3. Sliding criterion – Sliding evolution law

In the literature, Coulomb criterion is the most widely used frictional sliding criterion, either in its traditional (*see* for example, Andrieux *et al.*, 1986, Gambarotta and Lagomarsino, 1993, Horii and Nemat-Nasser, 1983, etc.) or modified (Curnier, 1984) forms. This criterion is well suited to micromechanical models, since it is based on the calculation of the traction vectors on the mesocrack faces. On the contrary, the model described here deals with sliding γ on a macroscopic scale, in the same way as damage $\mathbf{D}$, despite their micromechanical interpretations. Subsequently, the generalized notation with superscript k ($k = 1, 2, 3$) is used.

3.3.1. *Reversibility domain*

In the same manner as for $\mathbf{F}^D$, the force $\mathbf{F}^{\gamma k}$ may be divided into two parts:

$$\mathbf{F}^{\gamma k} = \mathbf{F}^{\gamma TK} + \mathbf{F}^{\gamma Nk} \tag{32}$$

where $\mathbf{F}^{\gamma Nk}$ (resp. $\mathbf{F}^{\gamma Tk}$) is the part of $\mathbf{F}^{\gamma k}$ normal (resp. tangential) to the equivalent crack plane:

$$\mathbf{F}^{\gamma Tk} = \mathbf{F}^{\gamma k} - (\boldsymbol{\nu}^k.\mathbf{F}^{\gamma k}.\boldsymbol{\nu}^k)\,\boldsymbol{\nu}^k \otimes \boldsymbol{\nu}^k \tag{33a}$$

$$\mathbf{F}^{\gamma Nk} = (\boldsymbol{\nu}^k.\mathbf{F}^{\gamma k}.\boldsymbol{\nu}^k)\,\boldsymbol{\nu}^k \otimes \boldsymbol{\nu}^k \tag{33b}$$

Sliding is assumed to occur when the norm of the tangential part $\mathbf{F}^{\gamma Tk}$ of the thermodynamic force related to γ^k reaches a given threshold depending on the normal strain (rather than normal stress as for Coulomb's criterion, since $\mathbf{F}^{\gamma k}$ is here an implicit function of strain). The convex reversibility domain $h^k \leq 0$ is thus written in $\mathbf{F}^{\gamma k}$-space:

$$\begin{aligned} h^k(\mathbf{F}^{\gamma k}, \boldsymbol{\nu}^k.\boldsymbol{\varepsilon}.\boldsymbol{\nu}^k) &= h^k(\mathbf{F}^{\gamma k} - \mathbf{F}^{\gamma Nk}, \boldsymbol{\nu}^k.\boldsymbol{\varepsilon}.\boldsymbol{\nu}^k) \\ &= \sqrt{\frac{1}{2}\operatorname{tr}[(\mathbf{F}^{\gamma k} - \mathbf{F}^{\gamma Nk}).(\mathbf{F}^{\gamma k} - \mathbf{F}^{\gamma Nk})]} \\ &\quad + \rho\,\boldsymbol{\nu}^k.\boldsymbol{\varepsilon}.\boldsymbol{\nu}^k \leq 0 \quad \text{if} \quad \boldsymbol{\nu}^k.\boldsymbol{\varepsilon}.\boldsymbol{\nu}^k \leq 0 \end{aligned} \tag{34}$$

where ρ is a material constant representing a sort of strain-related friction coefficient in the space $(\mathbf{F}^{\gamma k}; \boldsymbol{\varepsilon})$.

The aspect of the sliding threshold $h^k = 0$ has been drawn for a single mesocrack set (for a fixed k) with normal in the x_3 direction (the only non-zero damage tensor component is D_3) in the strain plane (ε_{33}, ε_{13}) with $\varepsilon_{13} = \varepsilon_{23}$ and $\varepsilon_{11} = \varepsilon_{22} = -\nu\varepsilon_{33}$ (ν is the Poisson ratio). Damage is, for the moment, assumed to be constrained from propagating.

In Figure 3, the solid line represents the threshold for $\gamma^k = 0$, whereas for the dashed line, γ^k has a non-zero initial value.

Remark 1. – Figure 3 shows only a section corresponding to $\varepsilon_{23} = 0$ of the total surface. The threshold is in fact cone-shaped (with its axis parallel to the ε_{33}-axis).

Remark 2. – Note that sliding shifts the surface by the amount γ^k_{13}, thus acting like a sort of kinematic hardening rule.

Remark 3. – The slope of the cone depends on the damage intensity D_3 (the slope is inversely proportional to D_3) implying that a higher crack density favours sliding.

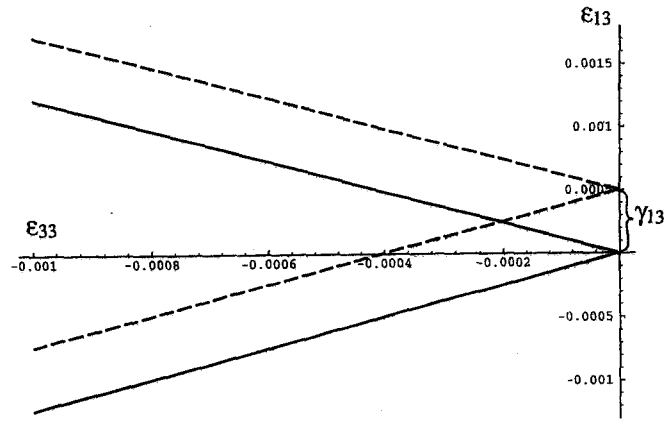

Fig. 3. – Sliding threshold in strain plane (ε_{33}, ε_{13}).

Remark 4. – Note that an alternative form of the frictional sliding criterion (34) can be obtained by replacing the normal strain $\boldsymbol{\nu}^k.\boldsymbol{\varepsilon}.\boldsymbol{\nu}^k$ by the invariant $\mathrm{tr}\,(\boldsymbol{\varepsilon}.\mathbf{D}^k)$. This substitution would lead to the slope not depending on the damage density. Experimental data should guide one to choose a particular form for a particular material.

Remark 5. – Due to the particular form of Equation (34), the vertex of the cone-shaped threshold is located on the axis $\varepsilon_{33} = 0$ with the ordinate γ_{13}^k. Condition (22) is fulfilled for any loading path, thus ensuring continuity of stress.

The same threshold has been drawn in the stress plane (σ_{33}, σ_{13}), assuming axisymmetric loading.

A hardening-like phenomenon is also observed on this cone-shaped curve. In conclusion, the threshold (34) leads to a yield surface similar to Coulomb's cone, but starting from an expression implying macroscopic quantities. In connexion with the opening/closure conditions for the mesocracks, the cone is shifted to the left (this corresponds to a negative normal stress at the closure point).

3.3.2. *Evolution law*

Many authors (*see*, for example, Michalowski and Mroz, 1978, Curnier, 1984) have pointed out that the slip rule associated with the standard Coulomb criterion in stress-space is not acceptable, since it would lead to a normal separating velocity. In the framework of the above criterion, no such paradox occurs: a standard scheme in the space of thermodynamic affinities related to γ^k is motivated by physical considerations. The normality rule appears to relate the frictional sliding evolution to the tangential part $\mathbf{F}^{\gamma Tk}$ of $\mathbf{F}^{\gamma k}$, indicating that sliding tends to occur in the crack plane (for a $\mathbf{D}^k$-proportional loading path). So the assumption of $\dot{\gamma}^k$-normality with respect to $h^k = 0$ is not contradictory:

(35)

$$\dot{\gamma}^k = \Lambda_\gamma^k \frac{\partial h^k\,(\mathbf{F}^{\gamma k} - \mathbf{F}^{\gamma Nk},\, \boldsymbol{\nu}^k.\boldsymbol{\varepsilon}.\boldsymbol{\nu}^k)}{\partial \mathbf{F}^{\gamma k}}$$

$$= \begin{cases} \mathbf{0} & \text{if} \quad h^k < 0 \text{ or } h^k = 0,\ \dot{h}^k < 0 \\ \Lambda_\gamma^k \left[\dfrac{\mathbf{F}^{\gamma Tk}}{\sqrt{2\,\mathrm{tr}\,(\mathbf{F}^{\gamma Tk}.\mathbf{F}^{\gamma Tk})}} \right] & \text{if} \quad h^k = 0 \text{ and } \dot{h}^k = 0 \end{cases} \quad , \quad \Lambda_\gamma^k \leq 0$$

3.3.3. *Identifiability of the model*

As already emphasized in the introduction, the model presented here has to be simple and efficient enough to be used in structural analysis. The small number (nine) of material parameters (λ, μ, α, β, C_0, C_1, g, B, ρ) is a first indication of the convenience of this formalism. Moreover, most of these parameters (seven exactly) are easily identified from classical axisymmetric triaxial compression tests with unloading: λ and μ are the conventional Lamé constants calculated from the range of the elastic response without damage growth; C_0, C_1 and g control the non-linear portion of the compression curves; and α and β are responsible for the longitudinal and transverse moduli degradation. Off-axis loading experiments are however necessary to determine B. For further details on the identification procedure, *see* Dragon *et al.*, 1994, and Pham, 1994. As far as the friction coefficient is concerned, it is easily related to the conventional coefficient ρ_c of Coulomb law ($|\sigma_{13}| + \rho_c \sigma_{33} = 0$), since ρ enters the expression of the slope of the sliding threshold in Figure 4. For the loading path considered above (Section 3.3.1),

$$\rho_c = \frac{\rho\mu}{|\beta| D_3 A} \quad \text{with} \quad A = \lambda(1 - 2\nu) + 2\mu - 2\alpha\nu D_3 \tag{36}$$

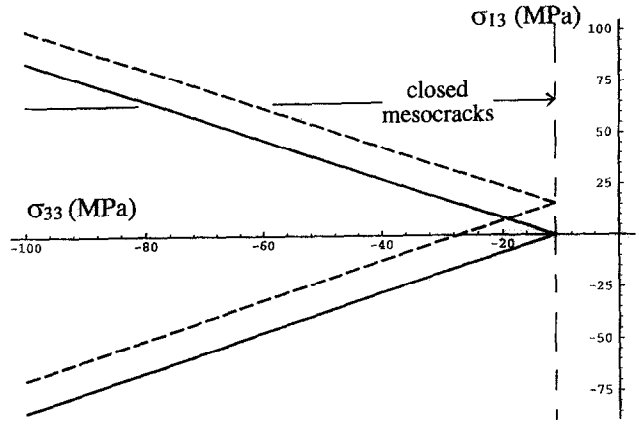

Fig. 4. – Sliding threshold in stress plane (σ_{33}, σ_{13}).

3.3.4. *Example*

The model with frictional sliding has been tested by simulating a basic loading path which emphasizes the genuine contribution of sliding. The constants employed in this simulation have been identified for Fontainebleau sandstone and listed in Table I; the friction coefficient (ρ = 5000 MPa) corresponds, for the damage density considered here, to a conventional Coulomb coefficient of about 0.5. The following homogeneous axisymmetric strain controlled loading path is considered:

TABLE I. – Parameters identified on Fontainebleau sandstone.

Parameters	λ [MPa]	μ [MPa]	α [MPa]	β [MPa]	g [MPa]	C_0 [MPa]	C_1 [MPa]	B [1]	ρ [MPa]
Sandstone	26250.	17500.	1900.	–20400.	–110.	0.001	0.55	0.	5000.

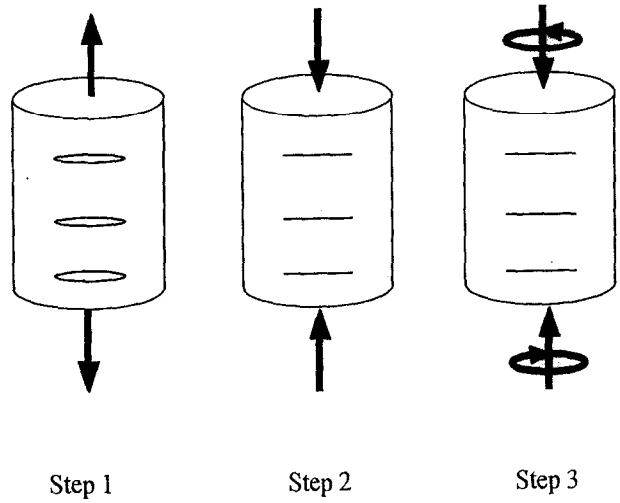

Fig. 5. – Steps of the homogeneous shear simulation.

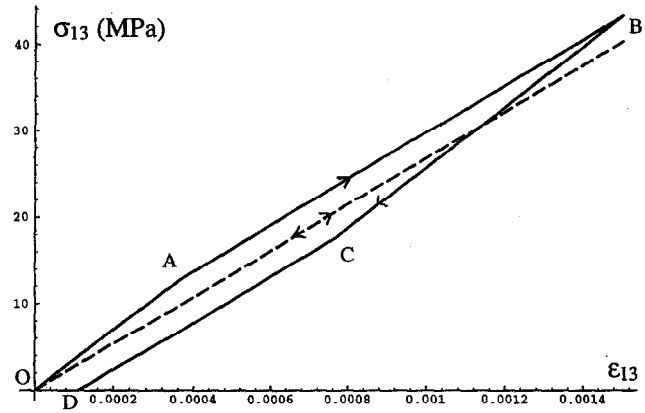

Fig. 6. – Stress–strain response for a shear simulation.

- Step 1: damaging tensile strain along vertical x_3 axis; generation of a set of parallel mesocracks normal in the x_3-direction.
- Step 2: unloading beyond crack closure.
- Step 3: ε_{11}, ε_{22}, ε_{33} remain constant, shear loading $\varepsilon_{13} = \varepsilon_{23}$ with axial unloading. **D** is assumed not to grow further.

Figure 6 represents σ_{13} vs. ε_{13} during Step 3 (solid line: model with frictional sliding; dashed line: model without friction).

In step OA, the closed mesocracks are "locked" by friction so that the solid behaves as undamaged ($\sigma_{13} = 2\mu\varepsilon_{13}$). Between A and B, the slope of the curve decreases due to crack sliding. The unloading starts with the phase BC in which no sliding occurs. Unlike step CD, in which energy is dissipated by frictional backsliding. This particular piecewise linear behaviour (due to sliding / no sliding) does not appear on the dashed curve; for the model without friction, cracks slide with no energy dissipation and no hysteresis loops are generated. Note that Figure 6 apparently represents a bilinear response, but the behaviour is dissipative (due to friction) along the segments AB and CD.

4. Damage/Sliding coupling

4.1. Damage criterion

The above frictional sliding model is valid for constant damage (or at least on $\mathbf{D}^k$-proportional loading paths). This paragraph aims to determine a damage criterion adapted for damage propagation in the tangential mode and to analyse the influence of changes of damage configuration on frictional sliding.

The damage evolution law described in Section 2 models splitting-like kinetics (the orientation of the mesocracks follows the ε^+-directions). For closed sliding mesocracks, damage undergoes the same kinetics, typical of brittle materials, as shown, for example, in Horii and Nemat-Nasser, 1985. Cracks branch towards the direction normal to the positive strain even in tangential frictional mode, as shown in Figure 7:

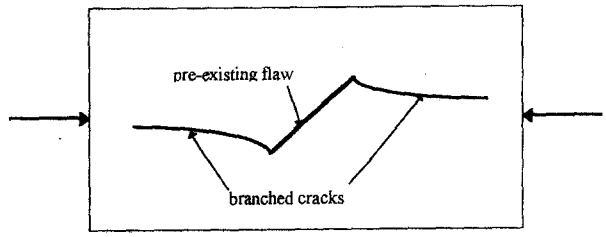

Fig. 7. – Schematization of crack branching mode under compressive loading.

Thus, the damage criterion (6) and the related evolution law (7) remain valid for closed sliding cracks. The form of this criterion has been drawn in the strain subspace $(\varepsilon_{33}, \varepsilon_{13})$ and the stress subspace $(\sigma_{33}, \sigma_{13})$. One proceeds as follows: a damage state is obtained after uniaxial tension along x_3 axis; from this state, radial loading paths are simulated in the strain subspace $(\varepsilon_{33}, \varepsilon_{13})$ in order to determine the points which satisfy the damage criterion (Figure 8). The components ε_{11} and ε_{22} are related to ε_{33} by Poisson's ratio ($\varepsilon_{11} = \varepsilon_{22} = -\nu\varepsilon_{33}$). So, for $\varepsilon_{33} < 0$, the considered loading paths correspond to simulations of uniaxial compression/torsion tests. The points are then transposed in the stress subspace $(\sigma_{33}, \sigma_{13})$ in Figure 9.

The dashed curve gives the criterion for mesocracks that slide without friction. The portion AA' (clockwise) of the curve corresponds to open cracks. The effect of sliding appears on AA' anticlockwise by "dilating" the threshold; this means that friction tends to strengthen the mesocracked solid.

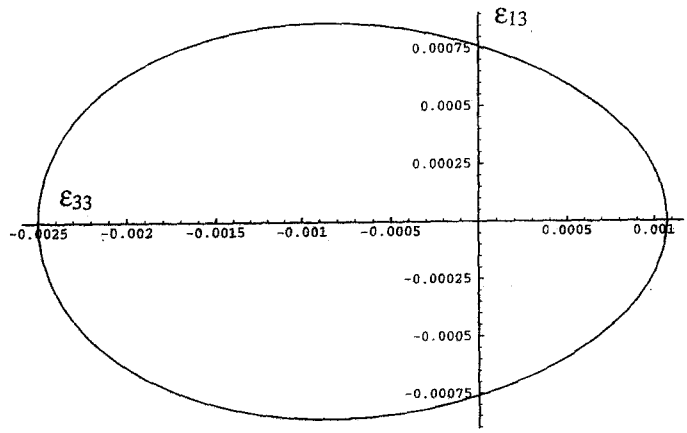

Fig. 8. – Damage criterion in strain plane $(\varepsilon_{33}, \varepsilon_{13})$.

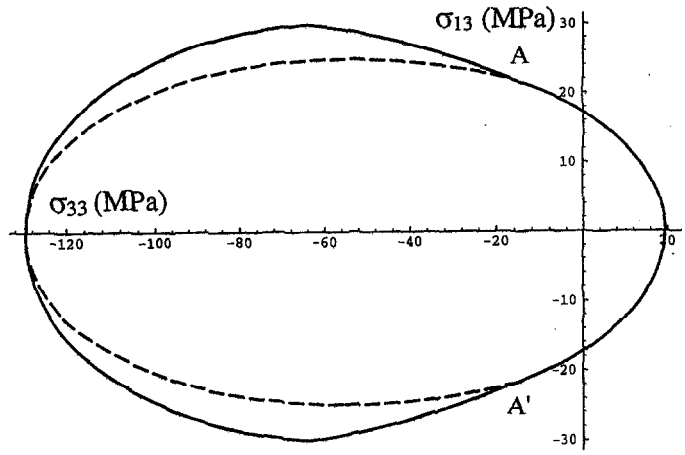

Fig. 9. – Damage criterion in stress plane (σ_{33}, σ_{13}).

4.2. Sliding evolution law

As far as sliding is concerned, Equations (34)-(35) have to undergo certain transformations: by construction, $\boldsymbol{\gamma}^k$ is initially "orthogonal" to $\mathbf{D}^k$ (*i.e.* $\boldsymbol{\gamma}^k : \mathbf{D}^k = 0$), but for $\mathbf{D}^k$-non-proportional loadings, the principal axes of $\mathbf{D}^k$ rotate and the condition $\boldsymbol{\gamma}^k : \mathbf{D}^k = 0$ is no longer verified. Keeping the same form for Equations (34)-(35) leads to discontinuities when the cracks open. The expression for this criterion has to account for the $\mathbf{D}^k$-axes rotation. Whereas extracting $\mathbf{F}^{\gamma Tk}$ from $\mathbf{F}^{\gamma k}$ led to the propagation of $\boldsymbol{\gamma}^k$ in the crack plane (*see* Section 3.3.2), employing a fraction of the normal part $\mathbf{F}^{\gamma Nk}$, indicates that damage, and then sliding, departs from the actual microcrack plane. This leads to the following partition of $\mathbf{F}^{\gamma k}$ (for a single crack of normal $\boldsymbol{\nu}^k$) with the introduction of a new entity $\mathbf{F}^k$:

$$\text{(37a)} \quad \mathbf{F}^{\gamma k} = \mathbf{F}^{\gamma Tk} + \mathbf{F}^{\gamma Nk} = \underbrace{\mathbf{F}^{\gamma Tk} + 4\beta\,(\boldsymbol{\gamma}^k : \mathbf{D}^k)\,\boldsymbol{\nu}^k \otimes \boldsymbol{\nu}^k}_{\mathbf{F}^k} - 4\beta\,(\boldsymbol{\varepsilon} : \mathbf{D}^k)\,\boldsymbol{\nu}^k \otimes \boldsymbol{\nu}^k$$

$$\text{(37b)} \quad = \quad \mathbf{F}^k \quad - 4\beta\,(\boldsymbol{\varepsilon} : \mathbf{D}^k)\,\boldsymbol{\nu}^k \otimes \boldsymbol{\nu}^k$$

and the equation for reversibility domain becomes:

$$\text{(38)} \quad h^k\,(\mathbf{F}^{\gamma k}, \boldsymbol{\nu}^k.\boldsymbol{\varepsilon}.\boldsymbol{\nu}^k) = h^k\,(\mathbf{F}^k, \boldsymbol{\nu}^k.\boldsymbol{\varepsilon}.\boldsymbol{\nu}^k) = \sqrt{\frac{1}{2}\,\mathrm{tr}\,(\mathbf{F}^k.\mathbf{F}^k)} + \rho\,\boldsymbol{\nu}^k.\boldsymbol{\varepsilon}.\boldsymbol{\nu}^k \leq 0$$

The associated evolution law gives:

$$\text{(39)} \quad \dot{\boldsymbol{\gamma}}^k = \Lambda_\gamma^k \frac{\partial\, h^k\,(\mathbf{F}^k, \boldsymbol{\nu}^k.\boldsymbol{\varepsilon}.\boldsymbol{\nu}^k)}{\partial \mathbf{F}^{\gamma k}}$$

$$= \begin{cases} \mathbf{0} & \text{if} \quad h^k < 0 \text{ or } h^k = 0,\ \dot{h}^k < 0 \\ \Lambda_\gamma^k \dfrac{\mathbf{F}^k}{\sqrt{2\,\mathrm{tr}\,(\mathbf{F}^k.\mathbf{F}^k)}} & \text{if} \quad h^k = 0 \text{ and } \dot{h}^k = 0 \end{cases}$$

Physically, the directional term in (39) means that sliding does not only occur in the crack plane but also has a normal component due to damage rotation.

Remark 1. – In the case of $\mathbf{D}^k$-proportional loading, $\mathbf{F}^k$ coincides with $\mathbf{F}^{\gamma Tk}$ and then Equations (38) and (34), and correspondingly Equations (39) and (35), are identical. Equations (34)-(35) thus represent a particular case of Equations (38)-(39).

Remark 2. – Although $\gamma^k : \mathbf{D}^k = 0$ is no longer valid when cracks rotate, no new invariant in terms of $\mathrm{tr}\,(\gamma^k.\mathbf{D}^k)$ or $\mathrm{tr}\,\gamma^k$ has been added to the strain energy w, since the above modified criterion is sufficient to avoid discontinuities that would appear at the onset damage rotation. Furthermore, the invariants that could enter $w\,(\varepsilon, \mathbf{D}, \gamma)$, e.g. $\mathrm{tr}\,\varepsilon\,\mathrm{tr}\,(\gamma^k.\mathbf{D}^k)$, $\mathrm{tr}\,\gamma^k\,\mathrm{tr}\,(\gamma^k.\mathbf{D}^k)$ or $\gamma^k : D_k\,\mathbf{L}^k : \gamma^k$, do not seem to provide more pertinent information about shear moduli degradation than the previous quantities, $\mathrm{tr}\,(\varepsilon.\gamma^k.\mathbf{D}^k)$ and $\mathrm{tr}\,(\gamma^k.\gamma^k.\mathbf{D}^k)$.

Remark 3. – The choice of the part of $\mathbf{F}^{\gamma Nk}$ entering $\mathbf{F}^k$ in Equation (38) is also justified by the required stress continuity: sliding crack opening leads to $\mathbf{F}^k = \mathbf{F}^{\gamma k} = \mathbf{0}$, *i.e.*:

$$\varepsilon.\mathbf{D}^k + \mathbf{D}^k.\varepsilon = \gamma^k.\mathbf{D}^k + \mathbf{D}^k.\gamma^k \tag{40}$$

and Equation (40), weaker than (22), allows to ensure the rank one for the jump $[[\mathbf{C}]]$, which occurs when passing from closed to open cracks, and the stress continuity.

To summarize this section, Equations (28)-(31) and (38)-(39) model the coupling of damage and friction. The energy is now dissipated by damage growth and/or friction:

$$\mathcal{D} = \mathbf{F}^D : \dot{\mathbf{D}} + \sum_{k=1}^{3} \mathbf{F}^{\gamma k} : \dot{\gamma}^k \tag{41}$$

Normality rules are assumed for the evolution of damage (7) and frictional sliding (39), thus satisfying the maximum dissipation principle (*see*, e.g., Simo and Ju, 1987, Govindjee *et al.*, 1995). However, in a normal dissipation framework, the criteria $f \leq 0$ (6) and $h \leq 0$ (34) are required to have additional properties: they have to be convex with respect to $\mathbf{F}^D$ (resp. $\mathbf{F}^{\gamma k}$) and to contain the origin. The expressions of f and h fulfil the former condition, however, due to the partitioning of the thermodynamic forces $\mathbf{F}^D$ and $\mathbf{F}^{\gamma k}$, the second condition can be violated (note here the obvious similarity with the Prager kinematic hardening rule). So, the algorithm of resolution has to check the non-negativity of $\mathcal{D}$ for each step and each integration point.

Integration of the model is performed numerically by discretizating the loading path in finite strain increments $\Delta\varepsilon$ and determining the state defined by ε, σ, $\mathbf{D}$ and γ^k at the end of each step:

- For each equivalent system, the normal strain $\nu^k.\varepsilon.\nu^k$ is checked.
- If $\nu^k.\varepsilon.\nu^k > 0$ (open cracks), γ^k vanishes and if $f = 0$ is attained, the evolution of $\mathbf{D}$ is calculated from Equation (7).
- If $\nu^k.\varepsilon.\nu^k < 0$ (closed cracks), both criteria $f = 0$ and $h^k = 0$ are checked; the increments $\Delta\gamma^k$ and $\Delta\mathbf{D}$ are simultaneously calculated by Equations (7) and (39). The integration of the two non-linear equations is performed by an implicit algorithm, whose numerical stability has been proved for elastoplastic models, *see* for example Ortiz and Popov, 1985. It has been confirmed for a class of damage models by Cormery, 1994, where, moreover, the implicit scheme appears to be naturally compatible with the actual constitutive formulation. Note the low degree of coupling between the two equations: γ^k only enters the second equation; thus, the evolution of $\mathbf{D}$ is fully and directly determined by the first relation (this corresponds to a "naturally implicit" resolution, *see* Cormery, 1994), whereas the calculation of γ^k requires an iterative procedure.

4.3. EXAMPLES

The same simulation as that described in Paragraph 3.3.4 has been carried out, with the difference that damage is allowed to progress. Figure 10*a* shows the shear stress-strain reponse (like in Figure 6). The solid line represents the model response with damage/friction coupling and the dashed line represents the response without friction. The material parameters are those listed in Table I.

In Figure 10*a*, two main factors distinguish the solid curve from the dashed one:

– at the very beginning, friction "locks" the mesocracks so that the initial slope for the solid curve is stronger than that for the dashed one.

– during unloading, the solid curve is characterized by two different slopes corresponding to a non-sliding phase followed by a sliding one, whereas the dashed curve has a constant slope.

Figure 10*b* gives the evolution of the components γ^k_{13} of the frictional sliding γ^k related to the initially formed crack system. From O to A, cracks are closed but do not slide. From A to C, frictional sliding occurs, which is accompanied by damage propagation between B and C. At point C, the system opens (the effects of sliding observed during unloading are due to emerging crack systems).

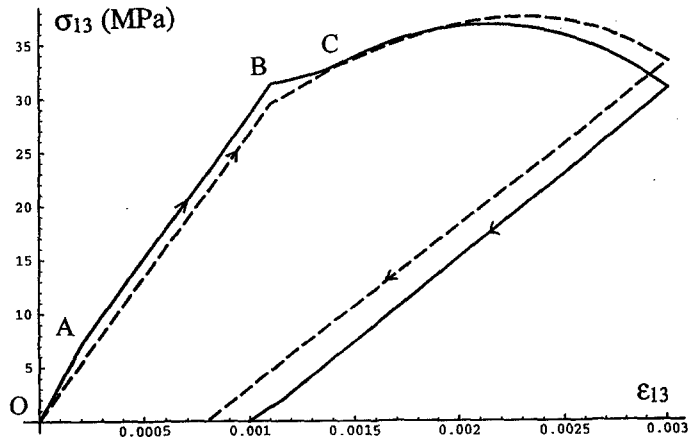

Fig. 10a. – Shear stress–strain response with damage/friction coupling.

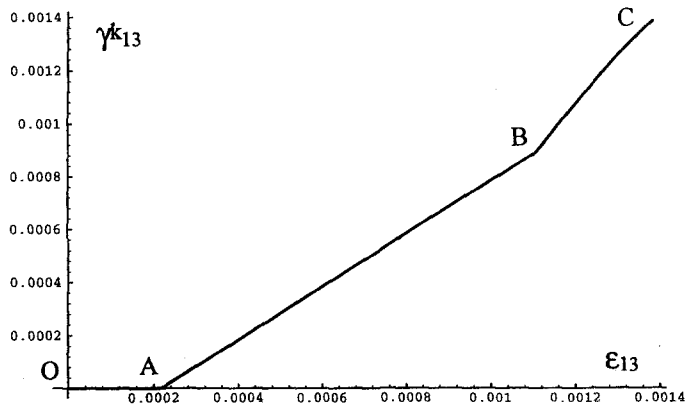

Fig. 10b. – Corresponding evolution of the sliding variable γ^k_{13} on the initial crack set.

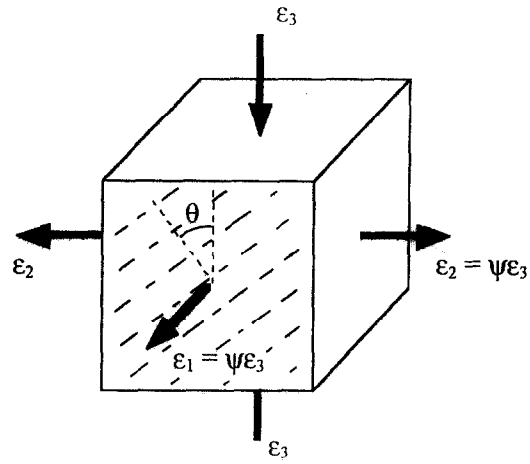

Fig. 11. – Compression-like loading.

The case of equioriented mesocracks undergoing a compression-like loading path has also been considered: the set of parallel cracks is defined by the angle θ between the crack normal and the direction of the axial strain ε_3 and the loading by the coefficient ψ ($\varepsilon_1 = \varepsilon_2 = \psi\varepsilon_3$, $\psi < 0$).

The simulation has been carried out for $\theta = 30°$ and $\psi = -0.3$. Figure 12 gives the axial deviatoric stress $\overline{\sigma}_3 = \sigma_3 - 1/3(\sigma_1 + \sigma_2 + \sigma_3)$ vs. the axial strain ε_3.

Note that the curve does not start at the axis origin because of the presence of mesocracks. There is then a residual macroscopic stress (for $\varepsilon_3 = 0$, $\sigma_3 \neq 0$). The mesocracks close and slide from the very beginning. Damage propagates from A to B. Unloading exhibits two main stages: from B to C, the mesocracks are locked by friction, whereas during the CO' phase the various equivalent systems progressively start to slide (this progressive activation is not observed on the non-frictional sliding dashed curve).

Remark. – The value of θ is the result of a compromise: θ has to be small enough to let the mesocracks close but large enough to let them slide.

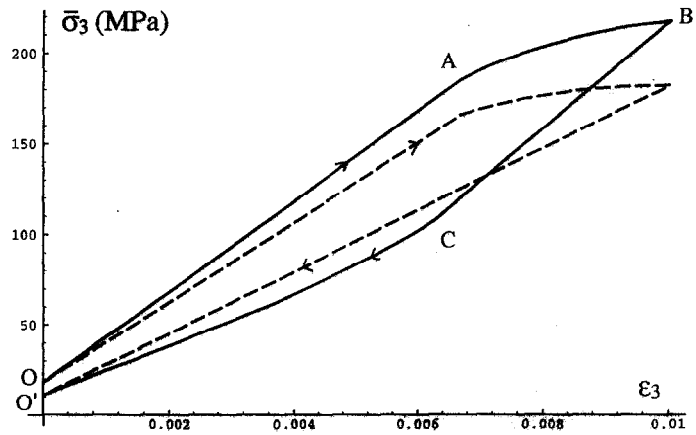

Fig. 12. – Stress–strain response for a compression-like simulation.

The simulation of the torsional test conducted by Pecqueur (*see* Figure 1) using the present model is given in Figure 13. One can see a reasonable qualitative correspondance with the experimental data, where a quasi-homogeneous loading is assumed, at least for the central third of the hollow cylinder (*see* Pecqueur, 1995).

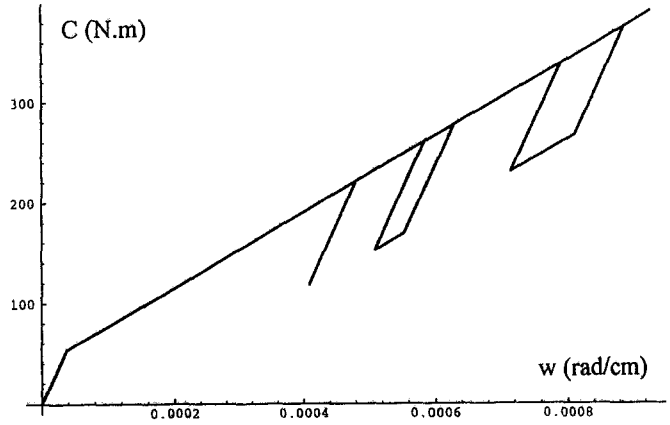

Fig. 13. – Model simulation of the torsional test by Pecqueur.

5. Conclusion

The model presented above accounts for two predominant dissipative mechanisms in brittle materials, namely damage growth and friction, and a number of related events, such a induced anisotropy, complex dissipative unloading curve, etc. The current model has three major advantages:

• It employs a tensorial damage variable and is formulated in a genuinely three-dimensional framework, unlike some existing approaches.

• Its modular nature allows it to treat independently the same problem at various levels of complexity:

First level - basic version (Dragon *et al.*, 1994) modelling the anisotropic degradation by mesocrack growth.

Second level - accounting for the normal moduli recovery (unilateral effect), which allows, for example, tension–compression cycles to be modelled.

Third level - introduction of frictional sliding (*i.e.* a sort of damage/plasticity coupling) to treat more complex loading paths (torsion, for example).

• In spite of the number of damage effects, such as anisotropy, dilatancy, frictional sliding and unilateral effect, the formulation of the equations remains simple enough for an efficient numerical approach for structural analysis.

Further work at the present time considers the frictional sliding as a viscous phenomenon and studies the consequences of frictional sliding on failure mechanisms via three dimensional localization. This work has already been developed for the basic version of the model, Dragon *et al.*, 1994.

APPENDIX

This Appendix contains expressions of the effective moduli in terms of material constants relevant to the damage model for basic loading paths (tension/shear, compression/shear). For further details and more general presentation of this issue, *see* Pham, 1994.

TENSION/SHEAR

Consider a single mesocrack set undergoing tension and shear loading (tension normal to the crack plane, *see* Figure 14).

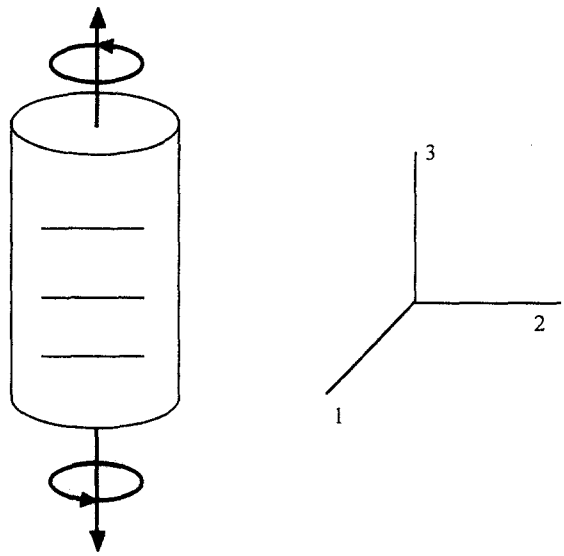

Fig. 14. – Tension/shear loading orthogonal to a single crack set.

Expressions of Young's modulus E_3, Poisson's ratio ν_{31} and shear modulus μ_{31} are:

$$E_3 = \lambda + 2\mu + 2(\alpha + 2\beta) D_3 - \frac{(\lambda + \alpha D_3)^2}{\lambda + \mu}$$

$$\nu_{31} = \frac{\lambda + \alpha D_3}{2(\lambda + \mu)}$$

$$\mu_{31} = \mu + \beta D_3$$

COMPRESSION/SHEAR LOADING

Consider now compressive and shear loading (compresion parallel to two equivalent crack systems, $D_1 = D_2$, *see* Figure 15).

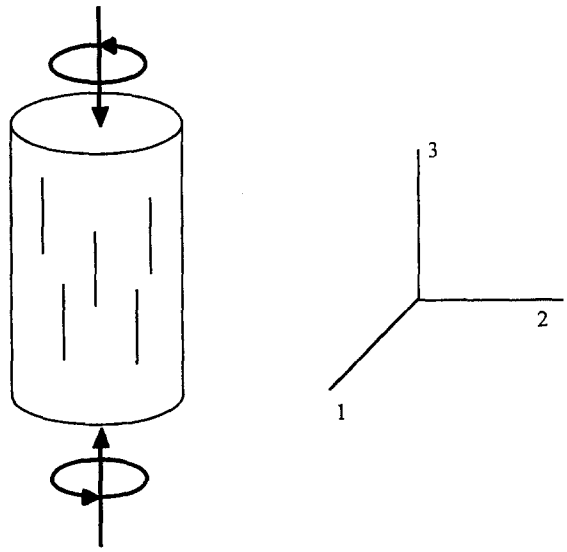

Fig. 15. – Compression/shear loading parallel to two crack systems.

Expression of Young's modulus E_3, Poisson's ratio ν_{31} and shear modulus μ_{31} are:

$$E_3 = \frac{(\lambda + 2\mu)\left[\lambda + \mu + 2(\alpha + \beta) D_1\right] - (\lambda + \alpha D_1)^2}{\lambda + \mu + 2(\alpha + \beta) D_1}$$

$$\nu_{31} = \frac{\lambda + \alpha D_1}{2\left[\lambda + \mu + 2(\alpha + \beta) D_1\right]}$$

$$\mu_{31} = \mu + \beta D_1$$

REFERENCES

ANDRIEUX S., 1981, Un modèle de matériau microfissuré avec frottement, *C. R. Acad. Sci. Paris*, t. 293, Série II, 329-332.

ANDRIEUX S., BAMBERGER Y., MARIGO J. J., 1986, Un modèle de matériau microfissuré pour les bétons et les roches, *J. Mécanique Théorique et Appliquée*, **5**, n° 3, 471-513.

CORMERY F., 1994, Contribution à la modélisation de l'endommagement par mésofissuration et du phénomène de localisation associé, PhD thesis, Univ. de Poitiers – ENSMA.

CURNIER A., 1984, A theory of friction, *Int. J. Solids Structures*, **20**, n° 7, 637-647.

CURNIER A., HE Q., ZYSSET P., 1995, Conewise linear elastic materials, *J. Elasticity*, **37**, 1-38.

DRAGON A., CORMERY F., DÉSOYER T., HALM D., 1994, Localized failure analysis using damage models, in *Localization and Bifurcation Theory for Soils and Rocks*, ed. R. CHAMBON *et al.*, pp. 127-140, Balkema, Rotterdam.

DRAGON A., HALM D., 1996, Modélisation de l'endommagement par mésofissuration : comportement unilatéral et anisotropie induite, *C. R. Acad. Sci. Paris*, t. 322, Série IIb, 275-282.

FOND C., BERTHAUD Y., 1995, Extensions of the pseudo tractions technique for friction in cracks, circular cavities and external boundaries; effect of the interactions on the homogenized stiffness, *Int. J. Fracture*, **74**, 1-28.

GAMBAROTTA L., LAGOMARSINO S., 1993, A microcrack damage model for brittle materials, *Int. J. Solids Structures*, **30**, n° 2, 177-198.

GOVINDJEE S., KAY G., SIMO J., 1995, Anisotropic modelling and numerical simulation of brittle damage in concrete, *Int. J. Num. Meth. Engng*, **38**, 3611-3633.

HALM D., DRAGON A., 1996, A model of anisotropic damage by mesocrack growth; unilateral effect, *Int. J. Damage Mechanics*, **5**, 384-402.

HORII H., NEMAT-NASSER S., 1983, Overall moduli of solids with microcracks: load-induced anisotropy, *J. Mech. Phys. Solids.*, **31**, n° 2, 151-171.

HORII H., NEMAT-NASSER S., 1985, Compression-induced microcrack growth in brittle solids: axial splitting and shear failure, *J. Geophys. Res.*, **90**, B4, 3105-3125.

JU J., 1991, On two-dimensional self-consistent micromechanical damage models for brittle solids, *Int. J. Solids Structures*, **27**, n° 2, 227-258.

KACHANOV M., 1982, A microcrack model of rock inelasticity – Part I: Frictional sliding on microcracks, *Mech. Mat.*, **1**, 19-27.

KACHANOV M., 1992, Effective elastic properties of cracked solids: critical review of some basic concepts, *ASME Appl. Mech. Rev.*, **45**, n° 8, 304-335.

KACHANOV M., 1993, Elastic solids with many cracks and related problems, in *Adv. Appl. Mech.*, **30**, ed. J. Hutchinson and T. Wu, pp. 259-445, Academic Press, New York.

KRAJCINOVIC D., BASISTA M., SUMARAC D., 1994, Basic principles, in *Damage Mechanics of Composite Materials*, ed. Talreja, pp. 1-51, Elsevier, Amsterdam – London – New York – Tokyo.

MICHALOWSKI R., MROZ Z., 1978, Associated and non-associated sliding rules in contact friction problems, *Arch. Mech.*, **30**, n° 3, 259-276.

ORTIZ M., POPOV E. P., 1985, Accuracy and stability of integration algorithms for elastoplastic constitutive relations, *Int. J. Num. Meth. Engng.*, **21**, 1561-1576.

PECQUEUR G., 1995, Étude expérimentale et modélisation du comportement d'une craie et d'un grès en torsion, PhD thesis, Univ. de Lille.

PHAM D. V., 1994, Suivi numérique des bandes de localisation dans les structures endommageables (endommagement par mésofissuration, anisotropie induite) – Applications en géomécanique, PhD thesis, Univ. de Poitiers – ENSMA.

SIMO J., JU J., 1987, Strain- and stress-based continuum damage models – I. Formulation, *Int. J. Solids Structures*, **23**, 821-840.

WESOLOWSKI Z., 1969, Elastic material with different elastic constants in two regions of variability of deformation, *Arch. Mech.*, **21**, n° 4, 449-468.

(Manuscript received November 14, 1996;
accepted April 10, 1997.)